Chest Lymph Node Anatomy

2

Ann T. Foran and Mukesh G. Harisinghani

2.1 Mediastinal Lymph Nodes

In 2009, a new lung cancer lymph node map was proposed by the International Association for the Study of Lung Cancer (IASLC) to reconcile the difference between the Naruke [1] and the Mountain–Dresler–American Thoracic Society (ATS) [2] maps and redefine the definitions of the anatomical boundaries of each lymph node station [3].

2.2 Supraclavicular Nodes 1

1R and 1L. *Low cervical, supraclavicular, and sternal notch nodes* (*see* Figs. 2.1, 2.2, 2.3, 2.4, and 2.5).

Upper border: Lower margin of cricoid cartilage.

Lower border: Clavicles bilaterally and, in the midline, the upper border of the manubrium; 1R designates right-sided nodes; 1L designates left-sided nodes in this region.

For lymph node station 1, the midline of the trachea serves as the border between 1R and 1L.

A. T. Foran
Department of Radiology, Beaumont Hospital, Dublin, Ireland
e-mail: foranat@tcd.ie

M. G. Harisinghani (✉)
Department of Radiology, Massachusetts General Hospital, Harvard Medical School, Boston, MA, USA
e-mail: mharisinghani@mgh.harvard.edu

M. G. Harisinghani (ed.), *Atlas of Lymph Node Anatomy*,
https://doi.org/10.1007/978-3-030-80899-0_2

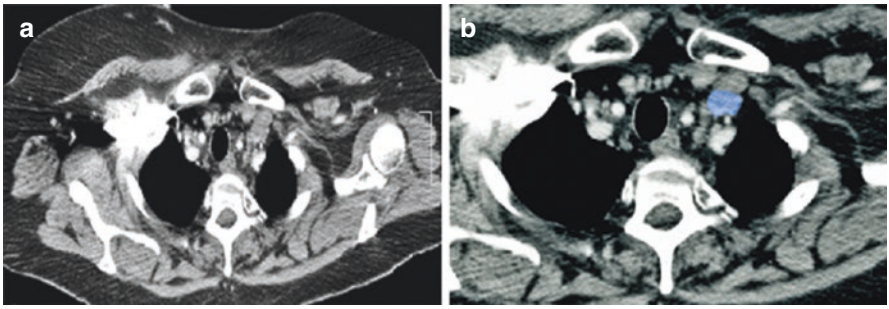

Fig. 2.1 (**a**, **b**) Axial CT scan through the lung apices shows enlarged left supraclavicular lymph node (*blue*)

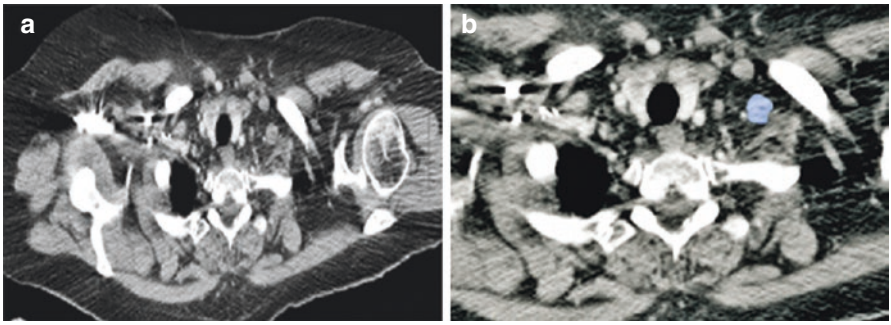

Fig. 2.2 (**a**, **b**) Axial CT scan through the lung apices shows enlarged left supraclavicular lymph node (*blue*)

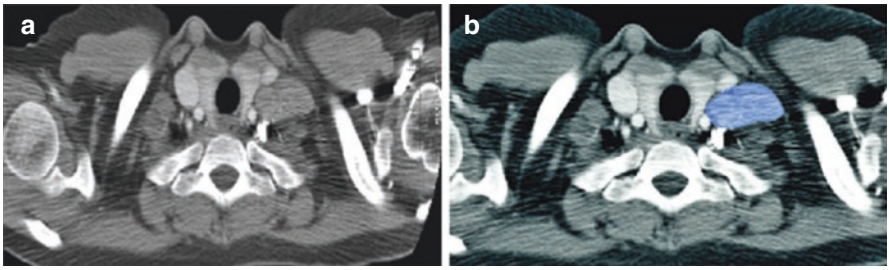

Fig. 2.3 (**a**, **b**) Axial CT scan through the lung apices shows enlarged left supraclavicular lymph node (*blue*)

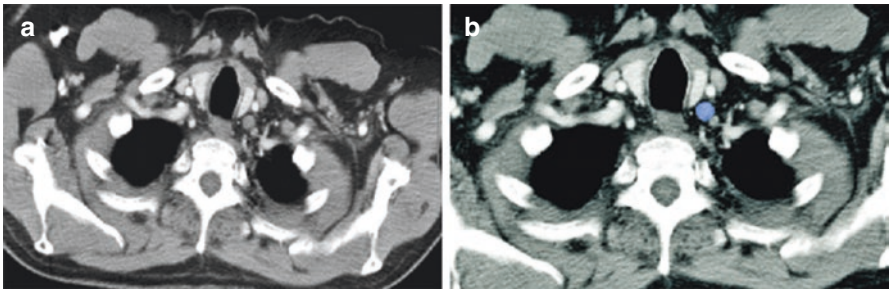

Fig. 2.4 (**a**, **b**) Axial CT scan through the lung apices shows enlarged left supraclavicular lymph node (*blue*)

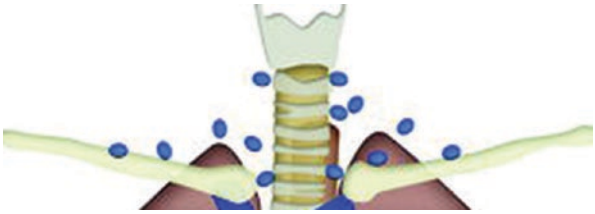

Fig. 2.5 Schematic diagram showing the anatomic locations of the low cervical, supraclavicular, and sternal notch node stations, which together comprise the supraclavicular lymph nodes

2.3 Superior Mediastinal Nodes 2–4

2R. *Upper paratracheal.* Includes nodes extending to the left lateral border of the trachea.

Upper border: Apex of the right lung and pleural space and in the midline, the upper border of the manubrium.

Lower border: Intersection of caudal margin of innominate vein with the trachea.

2L. *Upper paratracheal.*

Upper border: Apex of the left lung and pleural space and in the midline, the upper border of the manubrium.

Lower border: Superior border of the aortic arch (*see* Figs. 2.6 and 2.7).

3A. *Prevascular* (*see* Figs. 2.8, 2.9, and 2.10).

On the right:

Upper border: Apex of chest.

Lower border: Level of carina.

Anterior border: Posterior aspect of sternum.

Posterior border: Anterior border of superior vena cava.

On the left:

Upper border: Apex of chest.

Lower border: Level of carina.

Anterior border: Posterior aspect of sternum.

Posterior border: Left carotid artery.

3P. *Retrotracheal* (*see* Fig. 2.11).

Upper border: Apex of chest.

Lower border: Carina.

4R. *Lower paratracheal.* Includes right paratracheal nodes, and pretracheal nodes extending to the left lateral border of trachea (*see* Figs. 2.12, 2.13, and 2.14).

Upper border: Intersection of caudal margin of innominate vein with the trachea.

Lower border: Lower border of azygos vein.

4L. *Lower paratracheal.* Includes nodes to the left of the left lateral border of the trachea, medial to the ligamentum arteriosum.

Upper border: Upper margins of the aortic arch.

Lower border: Upper rim of the left main pulmonary artery.

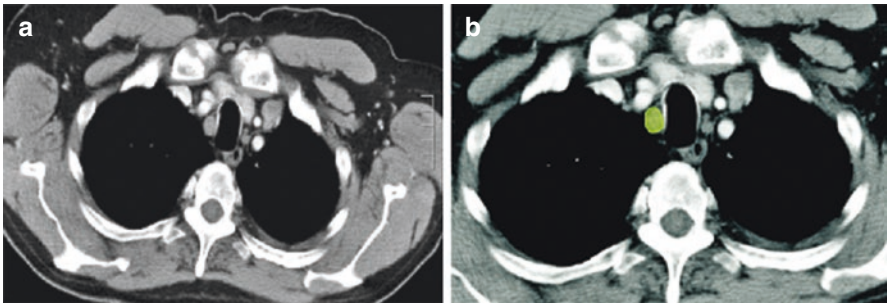

Fig. 2.6 (**a**, **b**) Axial CT scan showing an enlarged right upper paratracheal lymph node (*green*)

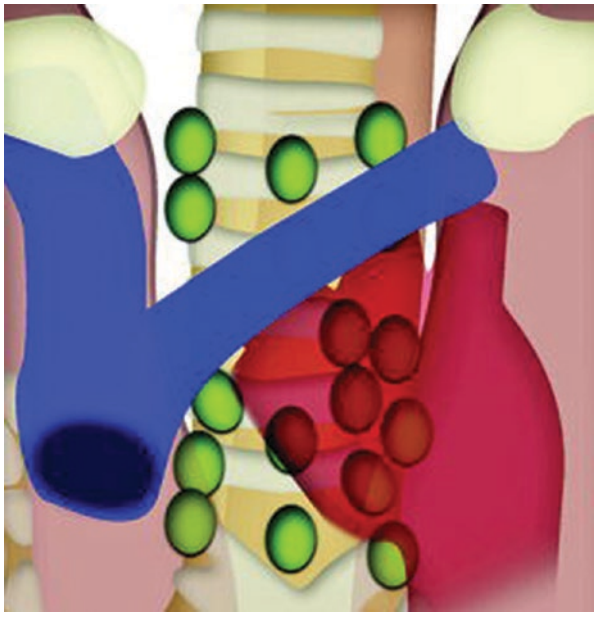

Fig. 2.7 Schematic illustration showing anatomic locations for paratracheal lymph nodes

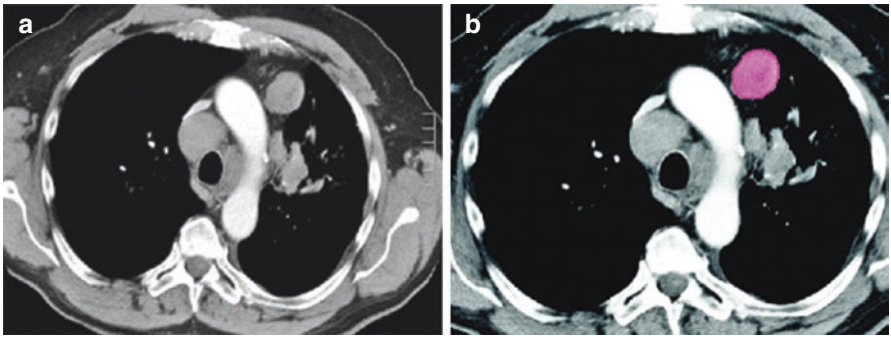

Fig. 2.8 (**a**, **b**) Contrast-enhanced axial CT scan shows an enlarged lymph node in the prevascular space on the left side, anterior to the arch of aorta (*red*)

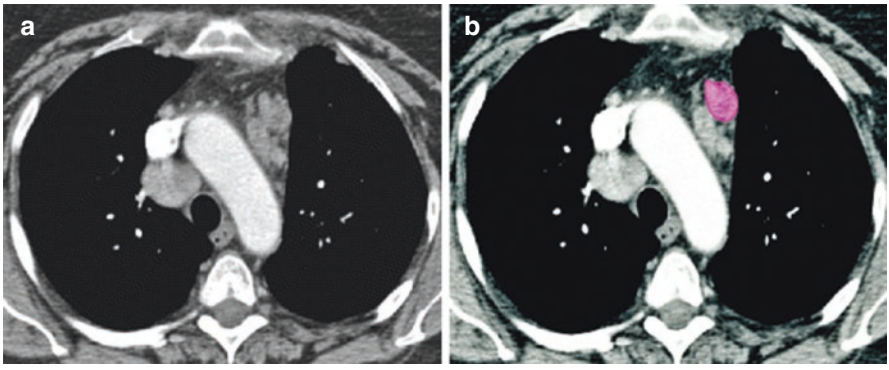

Fig. 2.9 (**a**, **b**) Contrast-enhanced axial CT scan shows an enlarged lymph node in the prevascular area on the left side, anterior to the descending aorta (*red*)

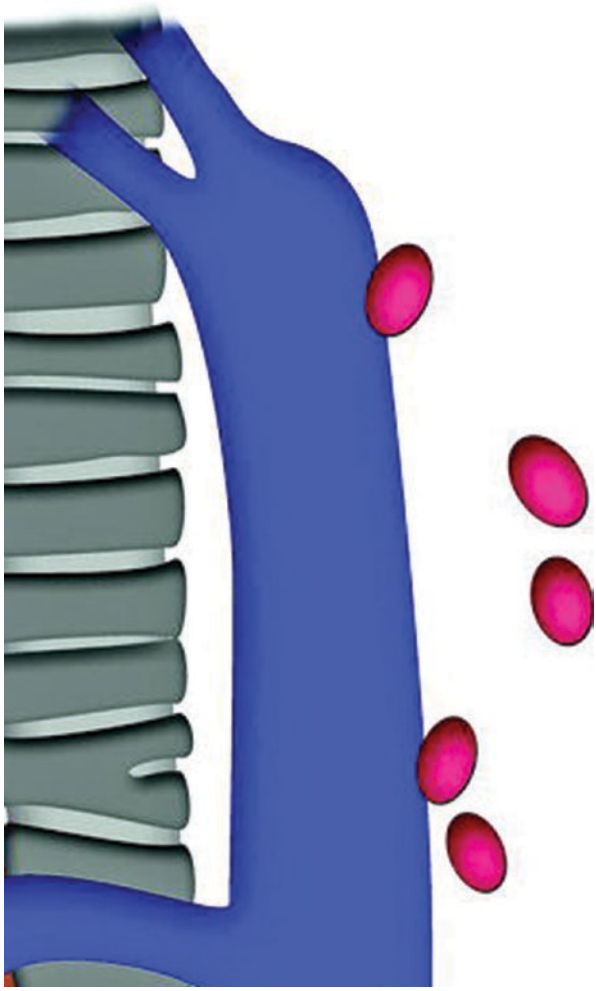

Fig. 2.10 Schematic illustration shows the anatomic location of prevascular group of lymph nodes

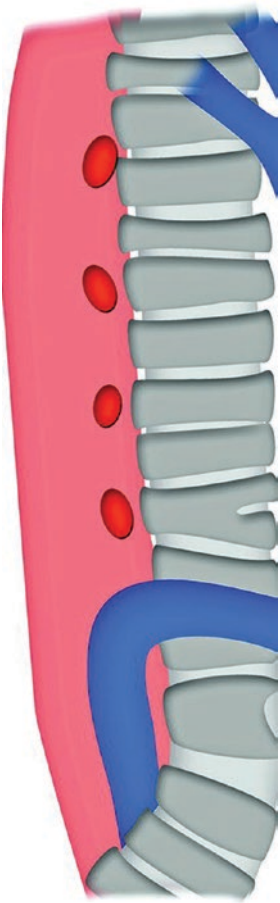

Fig. 2.11 Schematic illustration shows the anatomic location and distribution of retrotracheal group of lymph nodes (*dark red*)

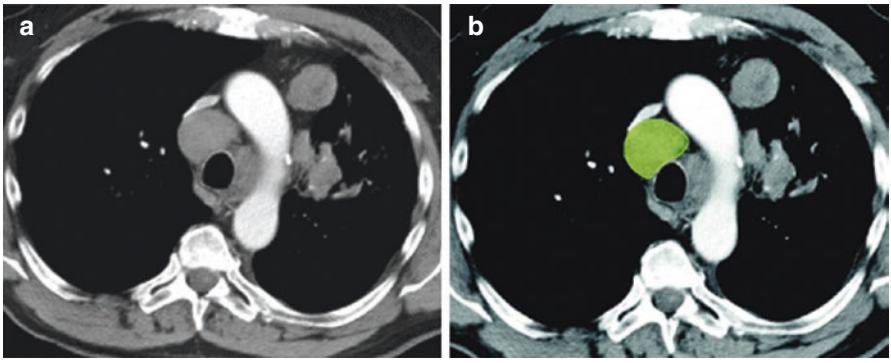

Fig. 2.12 (**a**, **b**) Axial contrast-enhanced CT image through the upper thorax shows an enlarged right-sided upper paratracheal lymph node (*green*)

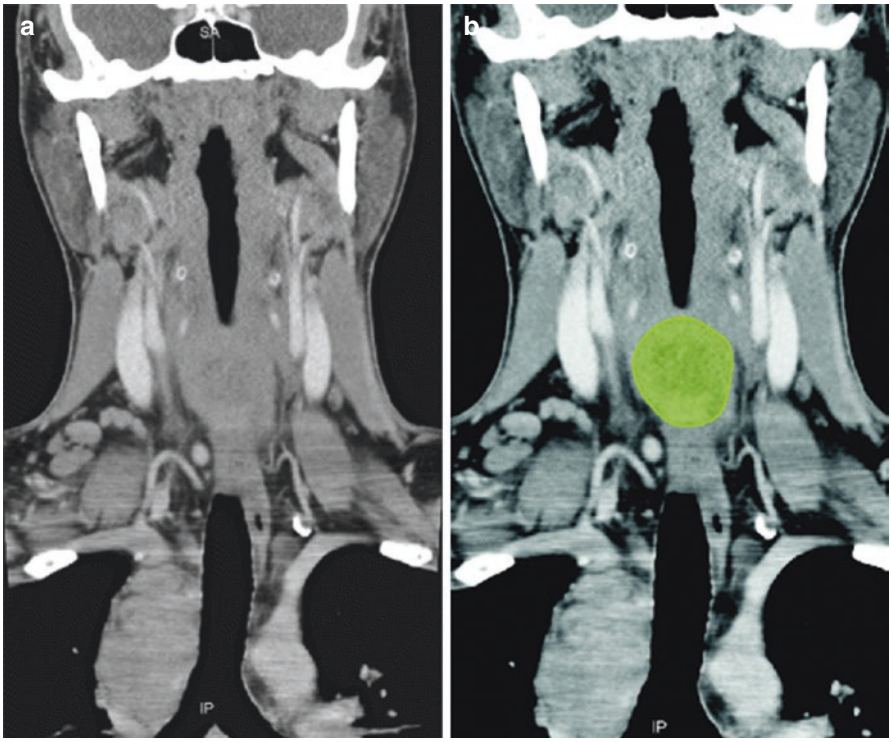

Fig. 2.13 (**a**, **b**) Coronal reformatted CT scan image of the same patient shows enlarged sternal notchl lymph node (*green*)

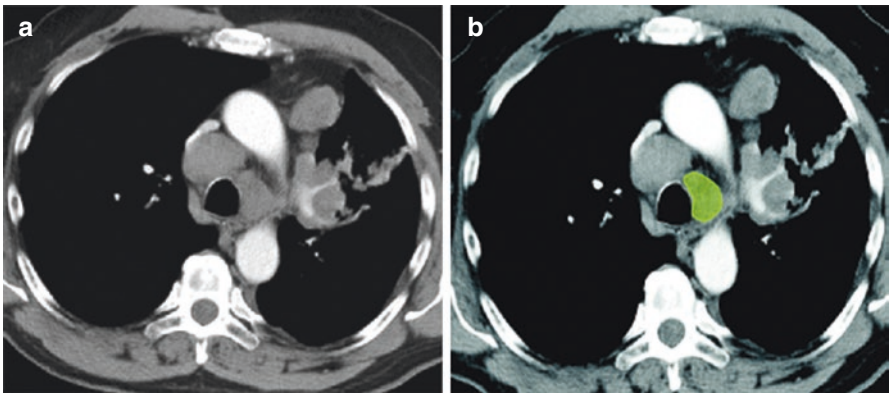

Fig. 2.14 (**a**, **b**) Axial contrast-enhanced CT scan through upper thorax shows an enlarged left lower paratracheal lymph node abutting the left lateral wall of the trachea (*green*)

2.4 Aortic Nodes 5–6

5. *Subaortic*. Lymph nodes lateral to the ligamentum arteriosum (*see* Fig. 2.15).
Upper border: The lower border of the aortic arch.
Lower border: Upper rim of the left main pulmonary artery.

6. *Para-aortic.* Lymph nodes anterior and lateral to the ascending aorta and aortic arch (*see* Figs. 2.16 and 2.17).
Upper border: A line tangential to the upper border of the aortic arch.
Lower border: The lower border of the aortic arch.

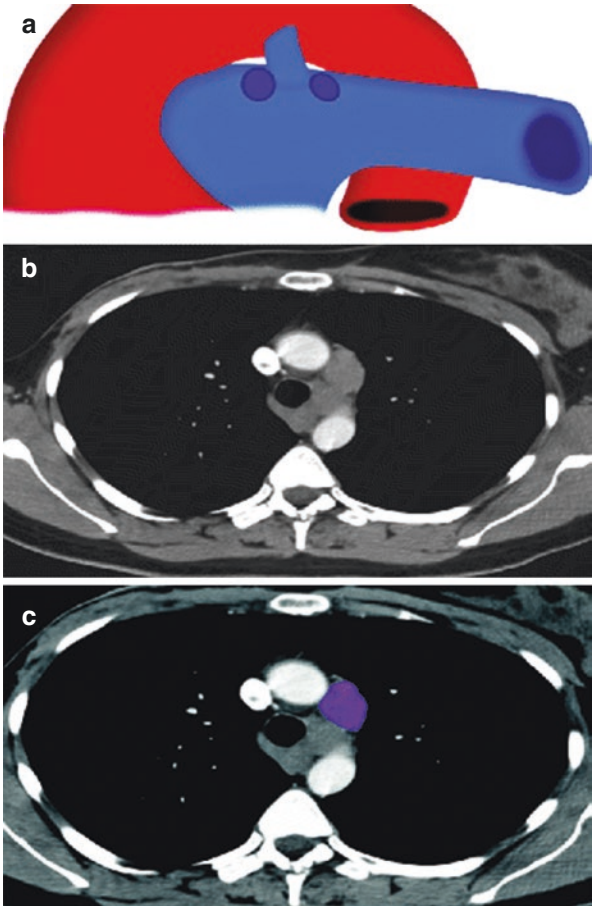

Fig. 2.15 (**a**) Schematic illustration shows the anatomic location of subaortic lymph nodes. (**b**, **c**) Axial contrast-enhanced CT scan image of the thorax shows an enlarged subaortic lymph node (*purple*)

Fig. 2.16 Schematic illustration shows the anatomic location for paraaortic group of lymph nodes

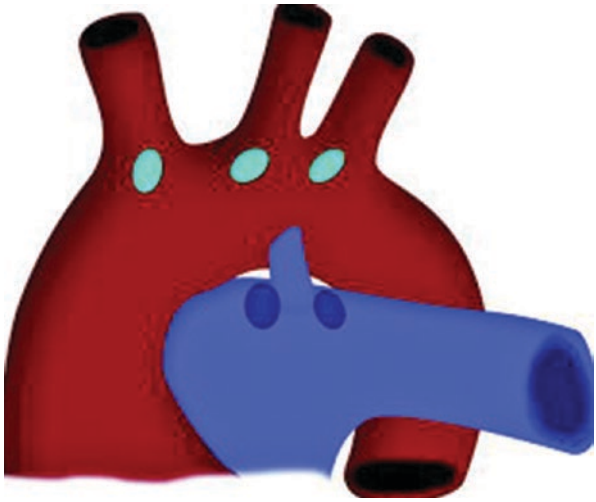

Fig. 2.17 Schematic illustration shows the anatomic locations of the para-aortic and retroaortic group of lymph nodes using color coding scheme

2.5 Inferior Mediastinal Nodes 7–9

7. *Subcarinal* (*see* Fig. 2.18).

Upper border: The carina of the trachea.

Lower border: The upper border of the lower lobe bronchus on the left; the lower border of the bronchus intermedius on the right.

8. *Paraesophageal.* Lymph nodes adjacent to the wall of the esophagus and to the right or left of the midline, excluding subcarinal nodes (*see* Figs. 2.19, 2.20, 2.21, and 2.22).

Upper border: The upper border of the lower lobe bronchus on the left; the lower border of the bronchus intermedius on the right.

Lower border: The diaphragm.

9. *Pulmonary ligament.* Lymph nodes lying within the pulmonary ligament (*see* Fig. 2.23).

Upper border: The inferior pulmonary vein.

Lower border: The diaphragm.

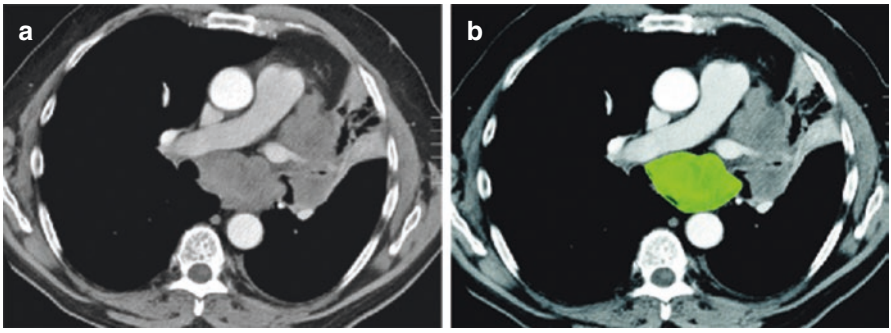

Fig. 2.18 (**a**, **b**) Axial contrast-enhanced CT scan of the thorax shows enlarged subcarinal group of lymph nodes (*green*)

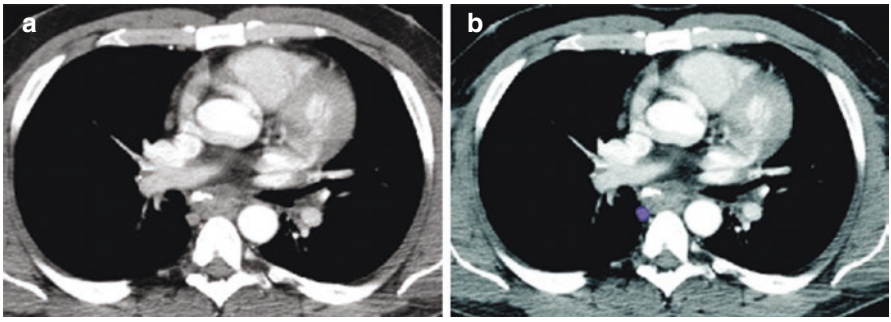

Fig. 2.19 (**a**, **b**) Axial contrast-enhanced CT scan of the thorax shows enlarged paraesophageal group of lymph nodes (*purple*)

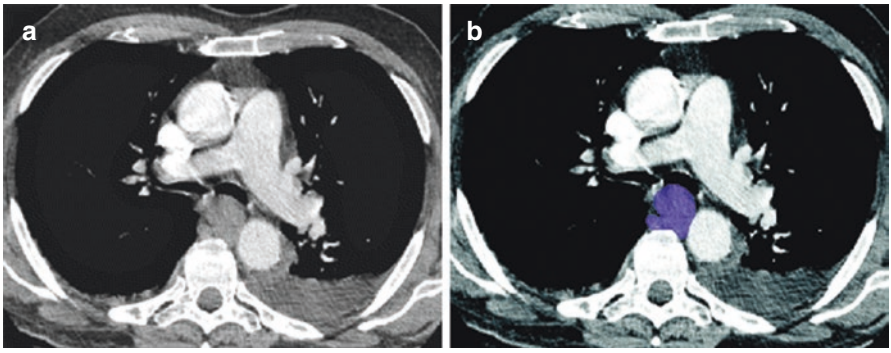

Fig. 2.20 (**a**, **b**) Axial contrast-enhanced CT scan of the thorax shows enlarged paraesophageal group of lymph nodes (*purple*)

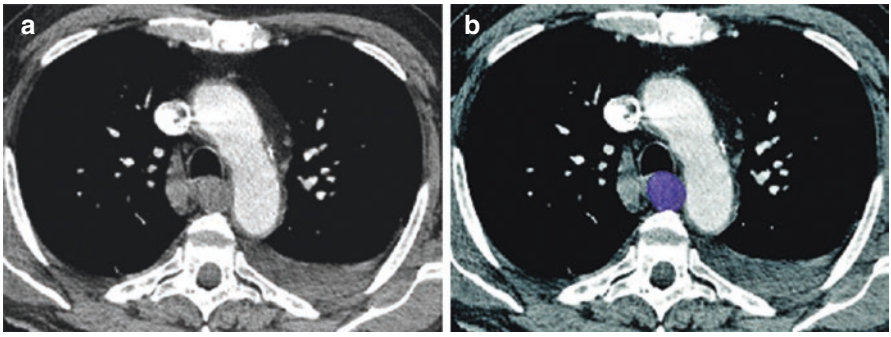

Fig. 2.21 (**a**, **b**) Axial contrast-enhanced CT scan of the thorax shows enlarged paraesophageal group of lymph nodes (*purple*)

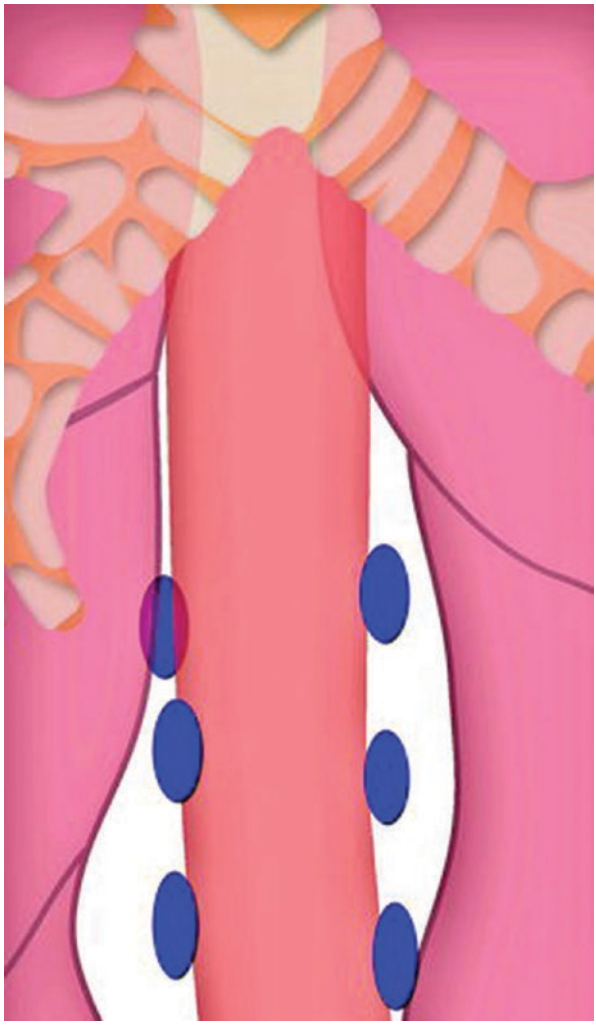

Fig. 2.22 Schematic illustration shows the anatomic location and distribution of the paraesophageal group of lymph nodes using color-coding scheme

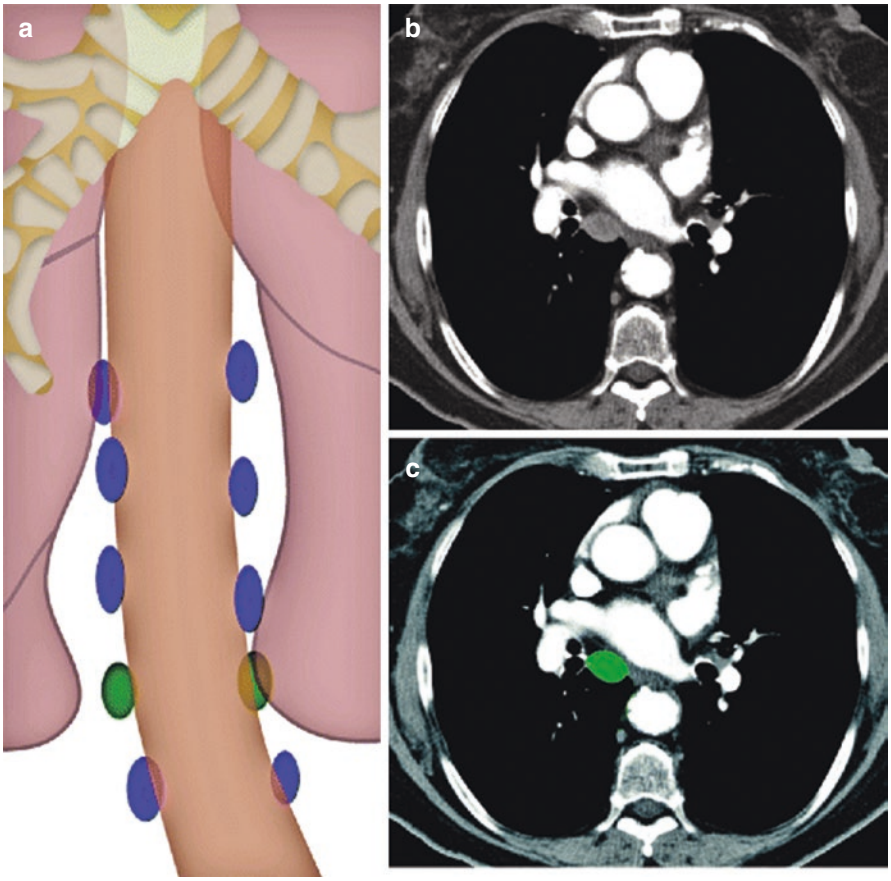

Fig. 2.23 (**a**) Schematic illustration shows the anatomic location and distribution of lymph nodes lying within the pulmonary ligament (*green*). These are seen interspersed between the paraesophageal group of lymph nodes (*violet*). (**b**, **c**) Axial contrast-enhanced CT scan of the thorax shows an enlarged right-sided pulmonary ligament lymph (*green*)

2.6 Hilar, Lobar, and (Sub)Segmental Nodes 10–14

These are all N1 nodes:

10. *Hilar.* Includes lymph nodes immediately adjacent to the mainstem bronchus and hilar vessels, including the proximal portions of the pulmonary veins and the main pulmonary artery (*see* Fig. 2.24).

Upper border: The lower rim of the azygos vein on the right; upper rim of the pulmonary artery on the left.

Lower border: Interlobar region bilaterally.

11. *Interlobar.* Between the origin of the lobar bronchi (*see* Fig. 2.25).

11R: on the right, which is subdivided into stations:
11Rs: Between the upper lobe bronchus and bronchus intermedius on the right.
11Ri: Between the middle and lower lobe bronchus on the right.
11L: on the left
12. *Lobar.* Adjacent to the lobar bronchi (*see* Fig. 2.26).
12R: on the right
12L: on the left
13. *Segmental*. Adjacent to the segmental bronchi.
13R: on the right
13L: on the left
14. *Subsegmental*. Adjacent to the subsegmental bronchi.
14R: on the right
14L: on the left

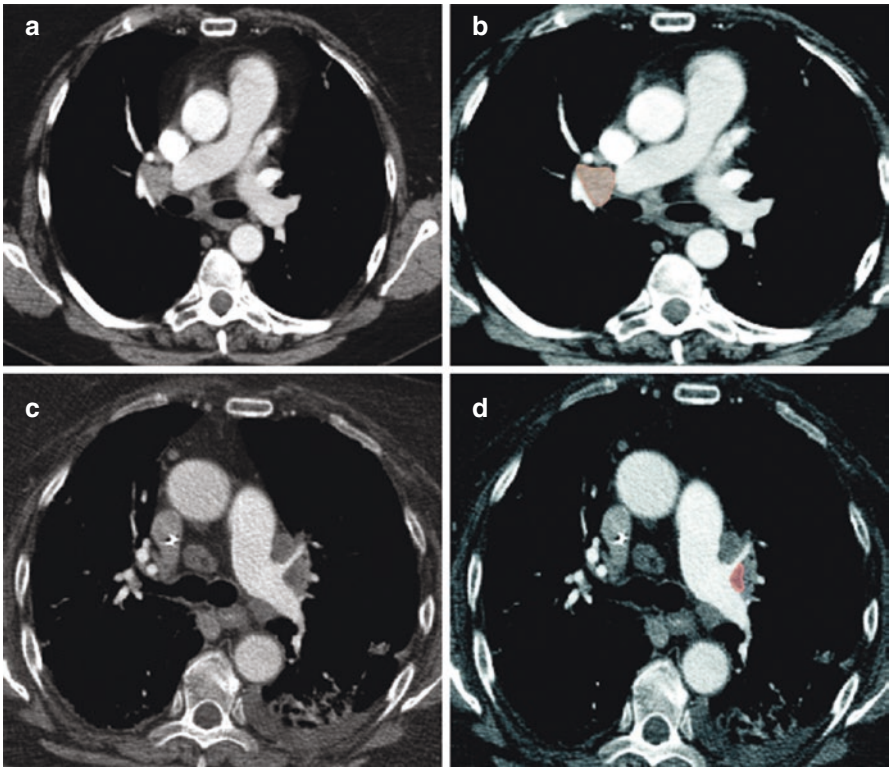

Fig. 2.24 (**a**, **b**) Axial contrast-enhanced CT scan of the thorax shows enlarged right hilar group of lymph nodes (*orange*). (**c**, **d**) Axial contrast-enhanced CT scan of the thorax shows enlarged left hilar group of lymph nodes (*orange*)

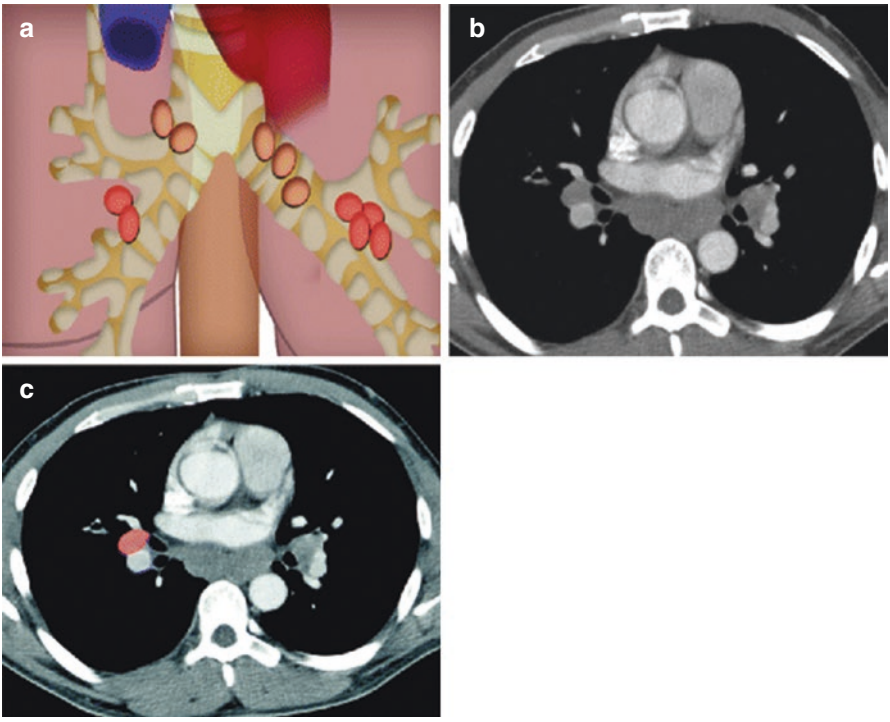

Fig. 2.25 (**a**) Schematic illustration shows the anatomic location and distribution of the hilar and interlobar group of lymph node. (**b**, **c**) An axial CT scan image of the thorax shows an enlarged right interlobar lymph node (*orange*)

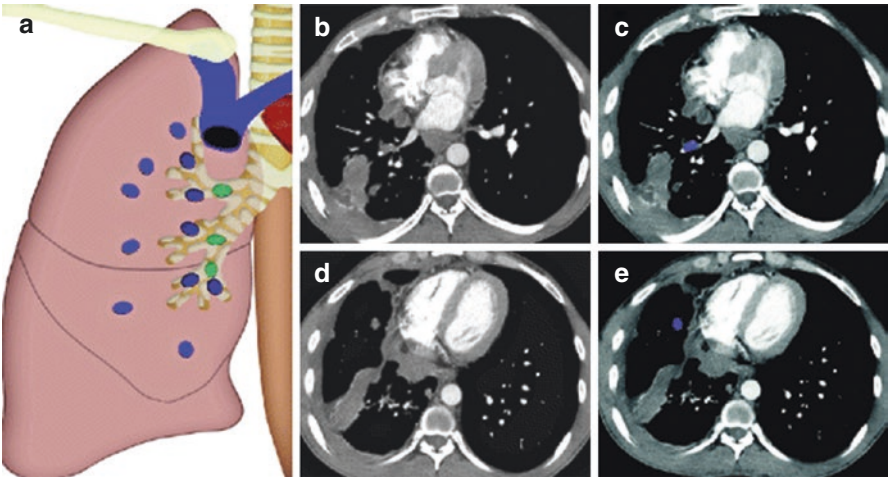

Fig. 2.26 (**a**) Schematic illustration shows the anatomic location and distribution of the lobar, segmental, and subsegmental group of lymph nodes using color-coding scheme. (**b**, **c**) Axial CT scan of the thorax shows an enlarged right segmental lymph node (*blue*). (**d**, **e**) Axial CT scan of the thorax shows enlarged right subsegmental lymph node (*blue*)

2.7 Malignant Causes of Enlargement

A study was performed to look at the appearance of the lymph node at CT to improve specificity for detecting malignant nodes in bronchogenic carcinoma. The four parameters evaluated were as follows: (1) node location, (2) homogenicity, (3) border delineation, and (4) delineation by fat. Twenty-one of 54 carcinoma patients had pathologically malignant nodes.. CT showed enlarged lymph nodes (>1 cm) in 20 of these (true-positive rate, 96%), but also in 13 of the 33 patients with pathologically benign lymph nodes (false-positive rate, 39%). A combination of all four CT parameters reduced the false-positive rate from 39% to 21% and decreased the true-positive rate from 96% to 86% [4].

The most common cause of malignant lymph node enlargement in the mediastinum is lung cancer. It has been reported that 20–25% of clinical stage I disease have mediastinal lymph node disease [5–7].

In patients with esophageal cancer, location of mediastinal lymph nodes depend on the location of the primary tumor. Thoracic mediastinal lymph nodes were involved in 19.44% of patients with upper thoracic esophageal carcinoma; in 34.7% of patients with middle thoracic esophageal carcinomas; and in 34.1% of patients with lower thoracic esophageal carcinoma [8].

Another cause of thoracic lymphadenopthy is lymphoma, in which mediastinal lymph node involvement is more frequent than hilar, which is usually asymmetrical and accompanied by mediastinal involvement [9] (*see* Figs. 2.27, 2.28, 2.29, 2.30, 2.31, and 2.32).

Lymphoma tends to expand along or around rather than invade existing structures. In Hodgkin's disease, upwards of 85% of patients have intrathoracic involvement on CT, compared with approximately 50% with non-Hodgkin's lymphoma [9, 10]. Hodgkin's disease tends to spread contiguously between lymph node groups, while non-Hodgkin's lymphoma more frequently involves atypical lymph node sites, such as posterior mediastinal and anterior diaphragmatic nodes [9, 10].

Intrathoracic lymph node metastases from extrathoracic carcinomas are infrequent. They were detected on chest radiograph in 25 of 1071 patients (2.3%) by McLoud and colleagues [11]. The primary malignancies included eight tumors of the head and neck, 12 genitourinary malignancies, three carcinomas of the breast, and two malignant lymphomas. The most frequently detected lymph node group was the right paratracheal 4R and 2R (60%).

Mabon and Libshitz [12] analyzed 50 mediastinal metastases of infradiaphragmatic malignancies on computed tomodensitography, a technique allowing a better visualization of all nodal groups in the mediastinum. Several lymph node stations were commonly involved, and only one single station was involved in only 6%. Besides a majority of genitourinary malignancies (kidney, 25; testis, 7; prostate, 4; ovary, 3; bladder, 2), they also observed metastases from carcinoma of the colon or rectum in 6 and stomach in 3. Libson and colleagues [13] reported 12 cases of mediastinal metastases in 19,994 patients (1%) with carcinomas of the stomach, pancreas, colon, and rectum.

In a recent study on the role of surgery in intrathoracic lymph node metastases from extrathoracic carcinoma [14], 26 of 565 patients with mediastinal lymph node enlargement had a history of extrathoracic carcinoma (breast, 7; kidney, 5; testis, 3; prostate, 2; bladder, 1; head and neck, 3; thyroid gland, 2; rectum, 1; intestine, 1; melanoma, 1).

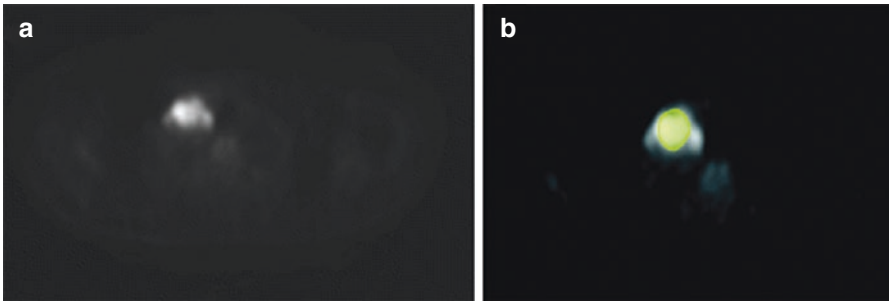

Fig. 2.27 (**a**, **b**) Axial positron emission tomography (PET) scan of the thorax shows fluorodeoxy-glucose (FDG) avid uptake by mediastinal lymph nodes in a case of lymphoma (*green*)

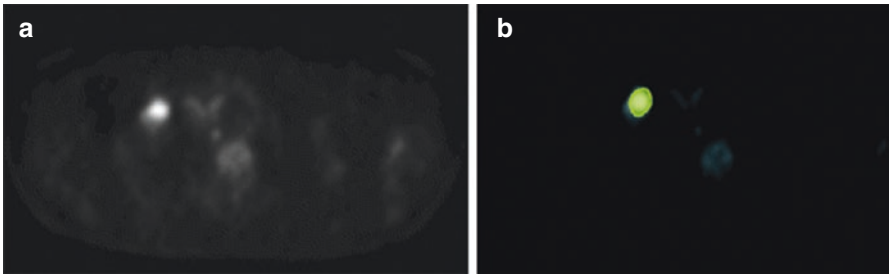

Fig. 2.28 (**a**, **b**) Axial PET scan of the thorax shows FDG avid uptake by mediastinal lymph nodes in a case of lymphoma (*green*)

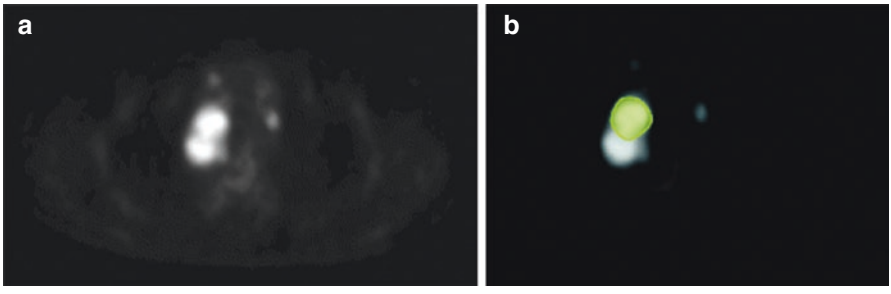

Fig. 2.29 (**a**, **b**) Axial PET scan of the thorax shows FDG avid uptake by mediastinal lymph nodes in a case of lymphoma (*green*)

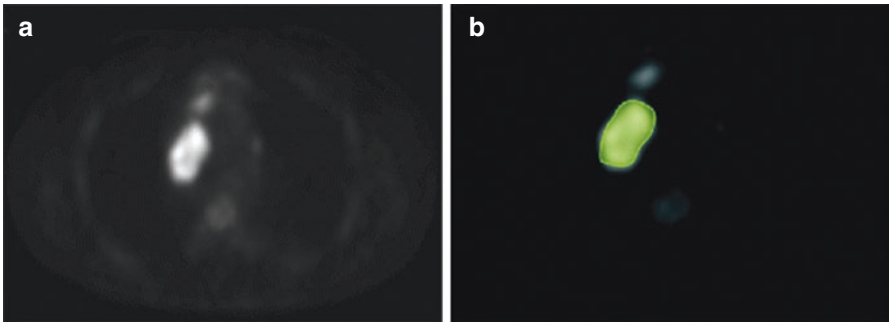

Fig. 2.30 (**a**, **b**) Axial PET scan of the thorax shows FDG avid uptake by mediastinal lymph nodes in a case of lymphoma (*green*)

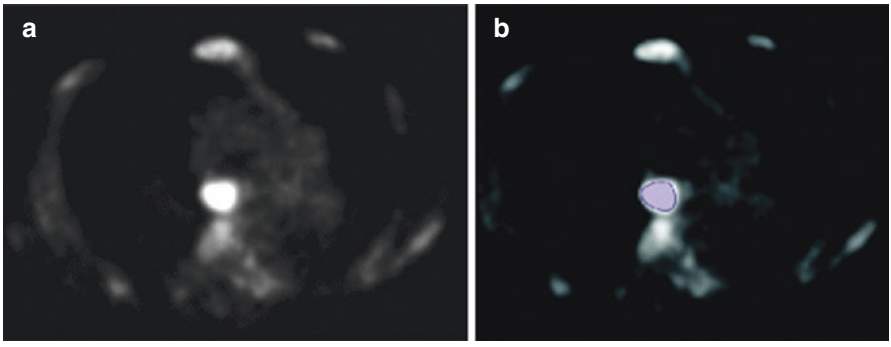

Fig. 2.31 (**a**, **b**) Axial PET scan of the thorax shows FDG avid uptake by mediastinal lymph nodes in a case of lymphoma (*purple*)

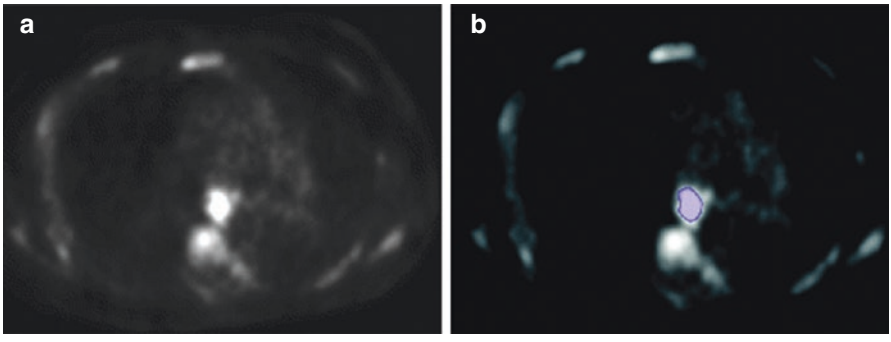

Fig. 2.32 (**a**, **b**) Axial PET scan of the thorax shows FDG avid uptake by mediastinal lymph nodes in a case of lymphoma (*purple*)

2.8 Axillary Lymph Nodes

Axillary lymph nodes are divided into five groups according to their afferent vessels and respective relationships with the vascular structures of the axilla [15] (*see* Figs. 2.33, 2.34, and 2.35).

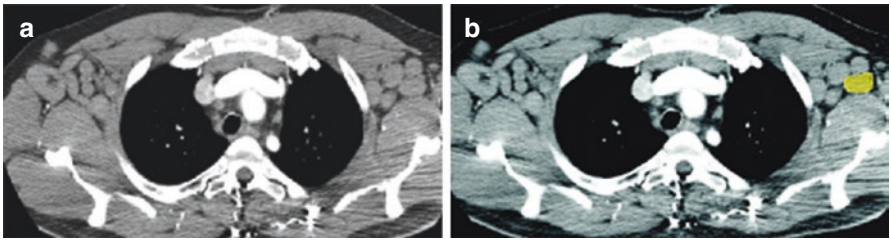

Fig. 2.33 (**a**, **b**) Axial contrast-enhanced CT scan of the thorax shows enlarged axillary group of lymph nodes (*yellow*)

Fig. 2.34 Schematic illustration shows different subgroups of the axillary lymph nodes using a color-coding scheme

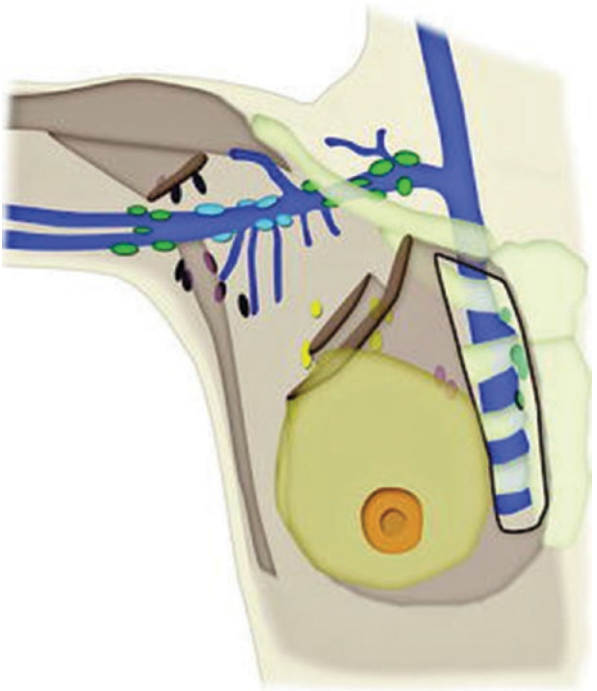

Fig. 2.35 Schematic illustration shows different subgroups of the axillary lymph nodes using a color-coding scheme

2.8.1 Lateral or Brachial Group

Nodes situated to the inferomedial side of the axillary vein.

Afferent vessels: Drain the lymph from the superficial and deep compartments of upper lymph, except for the superficial vessels of the arm that run along the cephalic vein.

Efferent vessels: Most terminate in the central or apical groups, whereas others pass into the supraclavicular nodes.

2.8.2 Anterior or Pectoral Group

Nodes located behind the pectoralis major muscle and along the lower border of the pectoralis minor, forming a chain along and behind the lateral thoracic vessels.

Afferent vessels: From the skin and muscles of the anterior and lateral walls of the trunk above the umbilicus, and the lateral parts of the breast.

Efferent vessels: Extend to the central and apical groups of axillary nodes.

2.8.3 Posterior or Subscapular Group

Nodes arranged in a chain that follows the subscapular vessels in the groove that separates the teres minor and subscapularis muscles.

Afferent vessels: Collect the lymph nodes arising from the muscles and skin of the back and from the scapular area down to the iliac crest.

Efferent vessels: Drain into the central and apical lymph nodes.

2.8.4 Central Group

Located in the central part of the adipose tissue of the axilla between the preceding chains that progressively converge toward them.

Efferent vessels: Extend into the apical group.

2.8.5 Apical Group

Nodes that occupy the apex of the axilla, behind the upper portion of the pectoralis minor and partly above this muscle. The majority of these nodes rest on the inferomedial side of the proximal part of the axillary vein, in close contact with the upper digitations of serratus anterior.

Afferent vessels: From all other axillary nodes; they also drain some superficial vessels running along the cephalic vein.

Efferent vessels: The efferent vessels of this group unite to form the subclavian trunk, which finally opens into the right lymphatic duct on the right side or into the thoracic duct on the left side.

The inferior border of the pectoralis major and the inferolateral and superomedial edges of the pectoralis minor can be used as anatomical landmarks to separate the inferior (I), middle (II), and superior (III) levels of the axillary space. Narrowing progressively, these levels contain the anterior (pectoral), lateral (brachial), posterior (subscapular), and central groups of nodes (level I), and then the central and apical groups (levels II and III).

2.8.6 Malignant Causes of Enlargement

The most common cause of malignant axillary lymph node enlargement is breast cancer. The relationship between the tumor diameter and the probability of nodal involvement in all tumor sizes appears linear. For patients with cancer 5 cm or greater, 71.1% are expected to have at least one node involved [16]. Other common causes include lymphoma and malignant melanoma.

Rare causes would include basal cell carcinoma [17] and ovarian cancer [18].

2.9 Chest Wall Nodes

2.9.1 Internal Mammary (Internal Thoracic or Parasternal) Nodes

These nodes lie at the anterior ends of the intercostal spaces, along the internal mammary (internal thoracic) vessels (*see* Figs. 2.36 and 2.37).

Afferent vessels: These nodes receive lymphatic drainage from the anterior diaphragmatic nodes, anterosuperior portions of the liver, medial part of the breasts, and deeper structures of the anterior chest and upper anterior abdominal wall.

Efferent vessels: May empty into the right lymphatic duct, the thoracic duct, or the inferior deep cervical nodes [19].

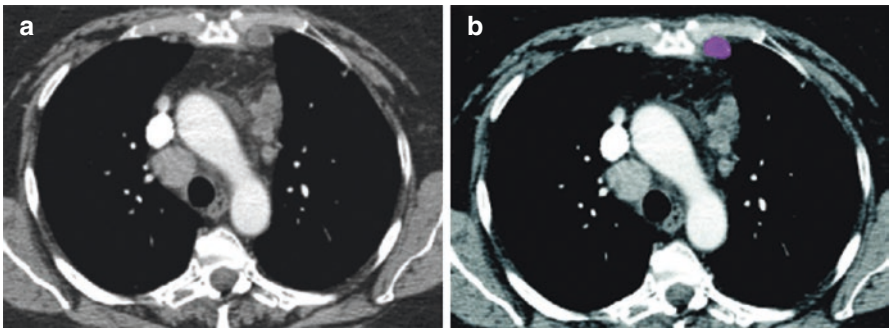

Fig. 2.36 (**a**, **b**) Axial contrast-enhanced CT scan of the thorax shows enlarged left internal mammary lymph nodes (*pink*)

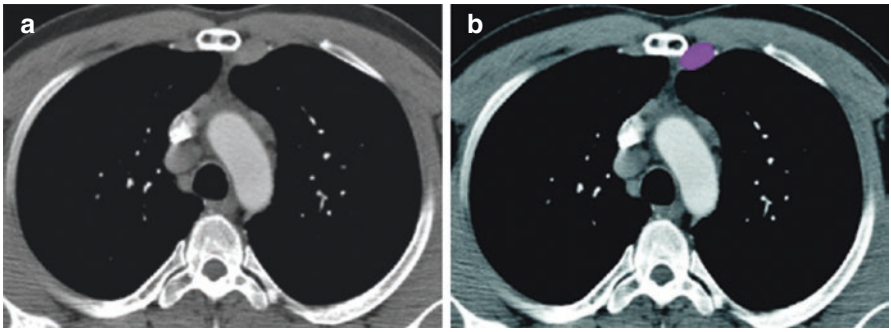

Fig. 2.37 (**a**, **b**) Axial contrast-enhanced CT scan of the thorax shows enlarged left internal mammary lymph nodes (*pink*)

2.9.2 Malignant Causes of Enlargement

One of the commonest causes of internal mammary lymph node enlargement is breast cancer. In a study on patients undergoing free flap breast reconstruction, 43 patients had internal mammary lymph node sampling and six patients had positive lymph nodes [20].

2.9.3 Posterior Intercostal Nodes

These nodes are located near the heads and necks of the posterior ribs.

Afferent vessels: They receive lymphatic drainage from the posterolateral intercostal spaces, posterolateral breasts, parietal pleura, vertebrae, and spinal muscles.

Efferent vessels: From the upper intercostal spaces end in the thoracic duct on the left, and in one of the lymphatic ducts on the right. Those from the lower four to seven intercostal spaces unite to form a common trunk, which empties into the thoracic duct or cisterna chyli [19].

2.9.4 Juxtavertebral (Pre-vertebral or Paravertebral) Nodes

These lie along the anterior and lateral aspects of the vertebral bodies, most common from T8 to T12. They communicate with posterior mediastinal lymph nodes and the posterior intercostal nodes, and similarly drain to the right lymphatic duct or thoracic duct [19].

2.9.5 Diaphragmatic Nodes

They are located on or just above the thoracic surface of the diaphragm and are divided into three groups [21].

2.9.6 Anterior (Pre-pericardial or Cardiophrenic) Group

These are located anterior to the pericardium, posterior to the xiphoid process, and in the right and left cardiophrenic fat (*see* Figs. 2.38, 2.39, 2.40, and 2.41).

Afferent vessels: From the anterior part of the diaphragm and its pleura, and the anterosuperior portion of the liver.

Efferent vessels: They drain to the internal mammary nodes alongside the xiphoid and can provide a route for retrograde spread of breast cancer to the liver via lymphatics of the rectus abdominis muscle when the upper internal thoracic trunks are blocked.

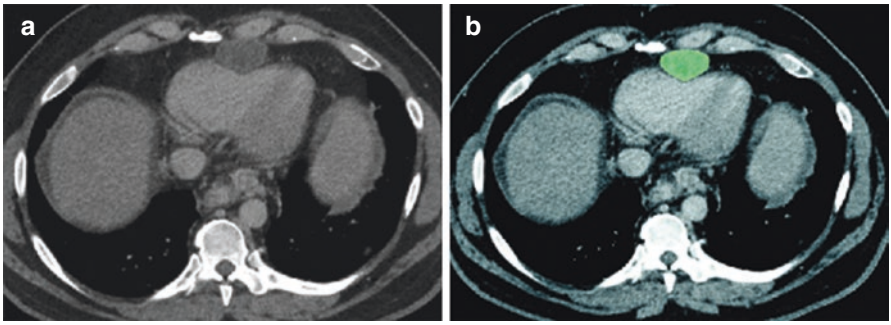

Fig. 2.38 (**a**, **b**) Axial contrast-enhanced CT scan of the thorax shows enlarged pericardial lymph node in a case of hepatocellular carcinoma (*green*)

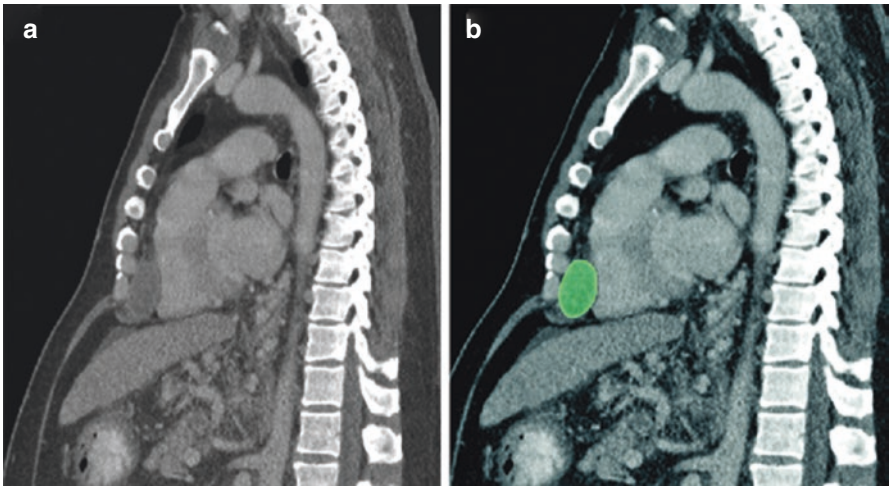

Fig. 2.39 (**a**, **b**) Sagittal reformatted CT scan of the thorax and upper abdomen shows enlarged pericardial lymph node in a case of hepatocellular carcinoma (*green*)

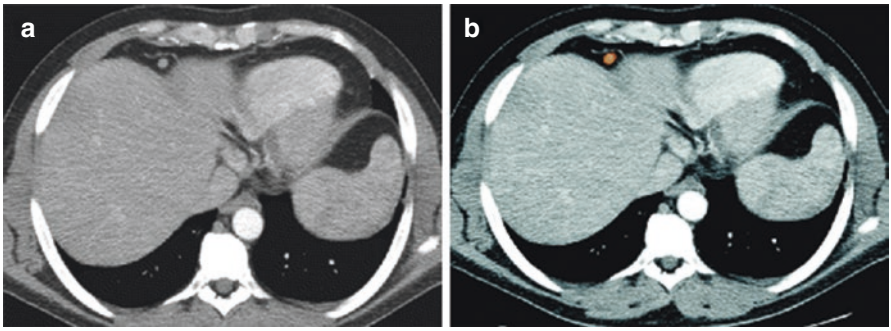

Fig. 2.40 (**a**, **b**) Axial contrast-enhanced CT scan of the thorax shows enlarged anterior diaphragmatic lymph node (*orange*)

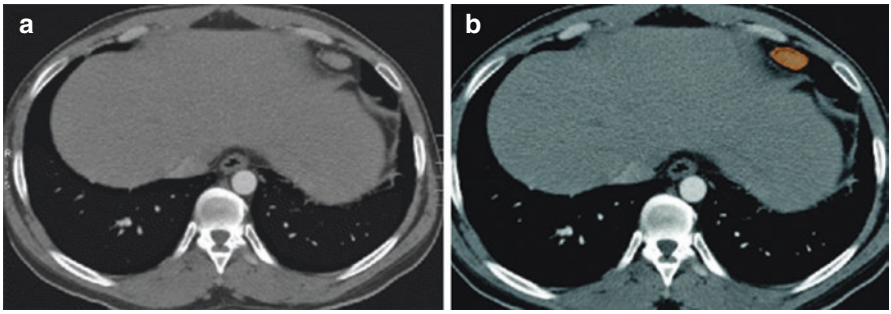

Fig. 2.41 (**a**, **b**) Axial contrast-enhanced CT scan of the thorax shows enlarged anterior diaphragmatic lymph node in a case of sarcoidosis (*orange*)

2.9.7 Middle (Juxtaphrenic or Lateral) Group

This group receives lymph from the central diaphragm and from the convex surface of the liver on the right.

2.9.8 Posterior (Retrocrural) Group

These nodes lie behind diaphragmatic crura and anterior to the spine.

Afferent vessels: Lymph from the posterior part of the diaphragm.

Efferent vessels: They communicate with the posterior mediastinal and paraaortic nodes in the upper abdomen.

Figure 2.42 represents the schematic illustration of all major groups of lymph nodes in the chest using a color-coding scheme. The color coding is also depicted on Fig. 2.43.

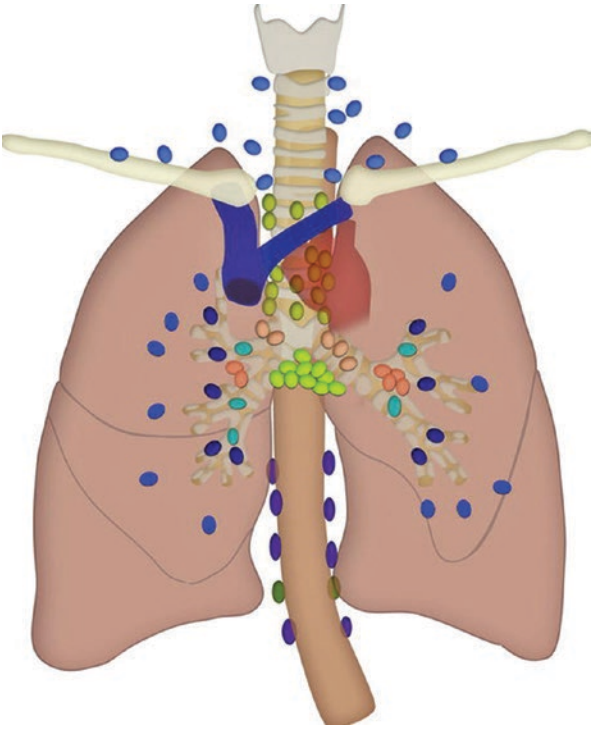

Fig. 2.42 Schematic illustration shows all major groups of lymph nodes in the chest using a color-coding scheme

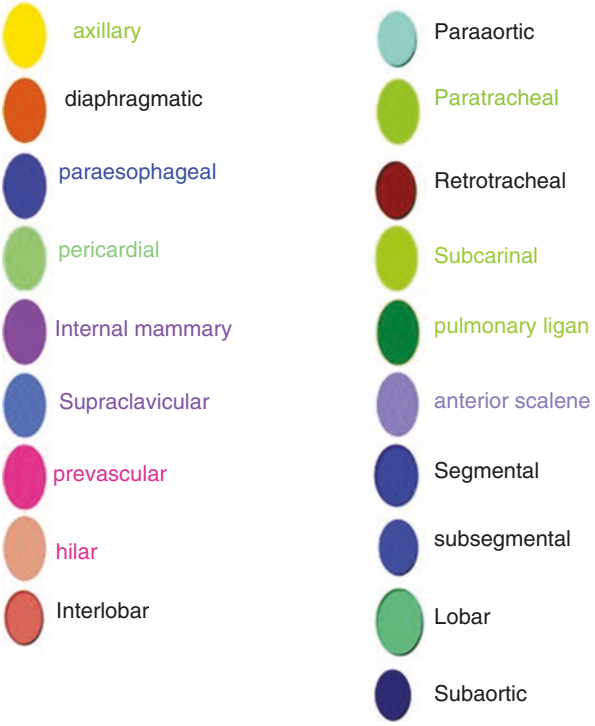

Fig. 2.43 Diagram showing the color-coding scheme used to identify various groups of lymph nodes in the chest

References

1. Naruke T, Suemasu K, Ishikawa S. Lymph node mapping and curability at various levels of metastasis in resected lung cancer. J Thorac Cardiovasc Surg. 1978;76:832–9.
2. Mountain CF, Dresler CM. Regional lymph node classification for lung cancer staging. Chest. 1997;111:1718–23.
3. Rusch VW, Asamura H, Watanabe H, Giroux DJ, Rami-Porta R, Goldstraw P, Members of IASLC Staging Committee. The IASLC lung cancer staging project: a proposal for a new international lymph node map in the forthcoming seventh edition of the TNM classification for lung cancer. J Thorac Oncol. 2009;4:568–77.
4. Feigin DS, Friedman PJ, Liston SE, Haghighi P, Peters RM, Hill JG. Improving specificity of computed tomography in diagnosis of malignant mediastinal lymph nodes. J Comput Tomogr. 1985;9:21–32.
5. Seely JM, Mayo JR, Miller RR, Muller NL. T1 lung cancer: prevalence of mediastinal nodal metastases and diagnostic accuracy of CT. Radiology. 1993;186:129–32.
6. Heavey LR, Glazer GM, Gross BH, Francis IR, Orringer MB. The role of CT in staging radiographic T1N0M0 lung cancer. AJR Am J Roentgenol. 1986;146:285–90.
7. Conces DJ Jr, Klink JF, Tarver RD, Moak GD. T1N0M0 lung cancer: evaluation with CT. Radiology. 1989;170(3 Pt 1):643–6.
8. Li H, Zhang Y, Cai H, Xiang J. Pattern of lymph node metastases in patients with squamous cell carcinoma of the thoracic esophagus who underwent three-field lymphadenectomy. Eur Surg Res. 2007;39:1–6.
9. Castellino RA, Blank N, Hoppe RT, Cho C. Hodgkin disease: contributions of chest CT in the initial staging evaluation. Radiology. 1986;160:603–5.
10. Castellino RA. The non-Hodgkin lymphomas: practical concepts for the diagnostic radiologist. Radiology. 1991;178:315–21.
11. McLoud TC, Kalisher L, Stark P, Greene R. Intrathoracic lymph node metastases from extrathoracic neoplasms. AJR Am J Roentgenol. 1978;131:403–7.
12. Mahon TG, Libshitz HI. Mediastinal metastases of infradiaphragmatic malignancies. Eur J Radiol. 1992;15:130–4.
13. Libson E, Bloom RA, Halperin I, Peretz T, Husband JE. Mediastinal lymph node metastases from gastrointestinal carcinoma. Cancer. 1987;59:1490–3.
14. Riquet M, Berna P, Brian E, Vlas C, Bagan P, Le Pimpec Barthes F. Intrathoracic lymph node metastases from extrathoracic carcinoma: the place for surgery. Ann Thorac Surg. 2009;88:200–5.
15. Lengele B, Hamoir M, Scalliet P, Gregoire V. Anatomical bases for the radiological delineation of lymph node areas. Major collecting trunks, head and neck. Radiother Oncol. 2007;85:146–55.
16. Carter CL, Allen C, Henson DE. Relation of tumor size, lymph node status, and survival in 24,740 breast cancer cases. Cancer. 1989;63:181–7.
17. Berlin JM, Warner MR, Bailin PL. Metastatic basal cell carcinoma presenting as unilateral axillary lymphadenopathy: report of a case and review of the literature. Dermatol Surg. 2002;28:1082–4.
18. Hockstein S, Keh P, Lurain JR, Fishman DA. Ovarian carcinoma initially presenting as metastatic axillary lymphadenopathy. Gynecol Oncol. 1997;65:543–7.
19. Suwatanapongched T, Gierada DS. CT of thoracic lymph nodes. Part I: anatomy and drainage. Br J Radiol. 2006;79:922–8.
20. Yu JT, Provenzano E, Forouhi P, Malata CM. An evaluation of incidental metastases to internal mammary lymph nodes detected during microvascular abdominal free flap breast reconstruction. J Plast Reconstr Aesthet Surg. 2011;64:716–21.
21. Aronberg DJ, Peterson RR, Glazer HS, Sagel SS. Superior diaphragmatic lymph nodes: CT assessment. J Comput Assist Tomogr. 1986;10:937–41.